BULGARIAN ACADEMY OF SCIENCES

CYBERNETICS AND INFORMATION TECHNOLOGIES • Volume **16**, No 5
Special Issue on Application of Advanced Computing and Simulation in Information Systems

Sofia • 2016 Print ISSN: 1311-9702; Online ISSN: 1314-4081
DOI: 10.1515/cait-2016-0056

Research on the Novel Method of Edge Detection Based on the Isotropic Diffusion Model and Total Variation Model

Xiaoming Wan

College of Information Engineering, Chongqing Industry Polytechnic College, Chongqing 401120, China
Email: 178189966@qq.com

Abstract: *A novel model of image segmentation based on watershed method is proposed in this work. To prevent the over segmentation of traditional watershed, our proposed algorithm has five stages. Firstly, the morphological reconstruction is applied to smooth the flat area and preserve the edge of the image. Secondly, multi-scale morphological gradient is used to avoid the thickening and merging of the edges. Thirdly, for contrast enhancement the top/bottom hat transformation is used. Fourthly, the morphological gradient of an image is modified by imposing regional minima at the location of both the internal and the external markers. Finally, a weighted function is used to combine the top/bottom hat transformation algorithm and the markers algorithm to get the algorithm. The experimental results show the superiority of the new algorithm in terms of suppression over segmentation.*

Keywords: *Novel method, Edge detection, The isotropic diffusion model, Total variation model.*

1. Introduction

Digital image processing technology originated in the 1920s and by the time of the early 1970s had formed a more perfected system of discipline. As they delved deeper into the subject, people came to realize the edges of the images contain the most useful information which is the main media of image information. It is significant to extract the edges of the images for image segmentation effectively, image recognition and so on. In the actual images, their qualities sometimes degenerate seriously as a result of noises. There is no doubt that studies about the mechanism of image degeneration, noise characters, how to establish the

degradation model, as well as how to restore effectively the images, will all benefit for the following edge detection work. Z h a n g et al. [5, 7] concentrate on the edge detection and the edge detection about digital image processing technologies. In edge detection aspect, we proposed an edge detection algorithm based on the directional wavelet transformation and an improved edge detection algorithm based on the Canny operator. In the edge detection aspect, an edge detection algorithm about the Gaussian noise image, based on the directional wavelet transformation and a restoring image algorithm about impulse noise, based on BP-net and adaptive window switching median filtering, is proposed. An Edge Detection Approach Based on Directional Wavelet Transform.

Z h a n g et al. [5, 7] propose an edge detection approach, based on directional wavelet transformation., which retains the separable filtering and the simplicity of computations and filter design from the standard two-dimensional WT. This separable discrete directional wavelet transform is implemented based on lattice theory. Although the transforms can be applied along any directions, only four transform directions {[1, 0], [0, 1], [1, 1], [–1, 1]} are chosen because of consideration of the computational complexity and correlation among pixels. In this new transform frame, the corresponding gradient magnitude is redefined. In the process of applying directional wavelet transforms along four directions {[1, 0], [1, 1], [0, 1], [–1, 1]}, the eight directions with respect to directional derivative are generated, namely {[1, 0], [–1, 0]; [1, 1], [–1, –1]; [0, 1], [0, –1]; [–1, 1],[1, –1]}. We find that it is unsuitable to apply non-maximum suppression only along maximal change direction of the derivatives in a number of experiments. In some cases, it is still necessary to choose the secondary change direction of the derivatives. Based on the analysis mentioned above, a new algorithm for non-maximum suppression is described. Improved Image Edge Extraction Algorithm Based on the Canny Operator. In the Canny edge detection algorithm, edges are detected and located by double threshold values, so that it is difficult to choose a reasonable lower limit threshold value. Choosing a big lower limit threshold will lead to troubles that edges cannot be fully located and are discontinuous; On the contrary, choosing a small lower limit threshold will produce a number of false edges. In addition, the edges which are gained by the traditional Canny algorithm cannot achieve the single pixel level, that is, An edge point corresponds to several responses. We have improved the Canny edge detection algorithm. Locate the edge by using a method with four threshold values. Then, conduct edge thin operation by introducing into a morphological operator. The improved algorithm can enhance capability of suppressing noise, delete false edges and obtain exact edges. Experimental results have indicated the feasibility and validity of the improved algorithm [3].

2. Introductions to image edge detection method

At present, wavelet edge detection has become one of the main image edge detection methods. Based on some understandings and summaries for the current wavelet de-noising literature, we introduce the threshold de-noising and the

relevance de-noising methods based on the standard wavelet respectively. Considering that the directional wavelet transform has more ability of directional transform than the traditional wavelet transform and the standard wavelet transform can be seen as a special case of the directional wavelet transform, we popularize the thoughts from the threshold de-noising and the relevance de-noising methods based on the standard wavelet into the directional wavelet. Our scheme is described as follows: Applying wavelet transforms along several directional combinations, and then letting median value of all groups as the final result, which can be considered as processing a rotating image. It is beneficial to eliminate the so called Gibbs affects and protect the image edges. In order to denoise impulse noises in images, an adaptive window switching median filtering method is proposed. It is different from the traditional median filtering method that our algorithm profits the thoughts from [84-91], adopt two step schemes including noise detecting and filtering to denoise. Since only noise pixels are filtered, it will help avoid serious degeneration of the restoration image. In the stage of the noise detection, a noise detection method based on BP-Net is proposed. Firstly, the BDND algorithm from [4] is improved, which acts as a weak classifier and applies an initial classification for each pixel; and then, a final decision is made by adopting the BP-Net. The method, based on two steps, helps the accuracy of the noise detector improve significantly, where the distribution of the impulse noise in 70% noise density can be detected effectively. In the stage of filtering, considering the traits of the noise detection method, a new adaptive window switching median filtering method is proposed. According to result of noise detection, the filter can adjust adaptively window's width and sample choicely, each noisy point in image is denoised by filtering. Two benefits are significant. Firstly, merely signal point involved in filtering treatment, which avoids the interference from the noise points during filtering process; secondly, the filter can adjust adaptively window's width, which can avoid the window is too large or too small to cause image blurring and distortion, protect effectively the edges and details of the images.

Since the edge contains a majority of information of image, edge detection is a critical step for image procession and analysis, which has significant influence on the characteristic description, matching and recognition after it. Incorporating the specific project of "Guidance technology based on the matching of optical reference image and infrared real-time image", this thesis concentrates on image edge detection technique research and its application. The paper M a, H u a n g and L i u [2] include: The fundamental theory of edge detection is reviewed, then, the main edge detection methods and some algorithmic evaluation standards are summarized. Based on analyzing the difficulty of edge detection, several problems in current edge detection research are indicated and the edge detection technique's direction is prospected. Considering that actual image edges are always diffused edges, diffuse edge detection is studied. Through analyzing the characteristics of diffuse edges and the difficulty of diffuse edge detection, and then reviewing former diffuse edge detection methods, we smooth out the noise at first, then weaken the edges' fuzziness to enhance the edges, so the edges can be similar to step edges, and finally adopt the traditional edge detection method to solve the problems of diffuse edge

detection. This algorithm uses fuzzy inference to synthesize the results of multilevel median filter and fuzzy weighted averaging filter, which can better preserve the image edges while smoothing out the mixed noise. As to the aspect of edge enhancement, several typical image enhancement methods are analyzed and compared from the view of reducing the edge fuzziness. Then, the shortcoming of morphological edge enhancement algorithm is discussed. Based on it, an adaptive fuzzy enhancement algorithm by edge width reduction is presented. This method can enhance the ramp edges by reducing edge width while smoothing noise out. Multi-scale edge detection is not only a hotspot of edge detection research but also one of its developmental directions. Therefore, an adaptive edge detection algorithm based on the Contourlet transform is proposed. This algorithm can do better than traditional wavelet shrinking edge detection algorithms in smoothing noise out and preserving edges and details. As to the aspect of multiscale edge detection, by analyzing that the common Laplacian Pyramid (LP) decomposition is not appropriate to capture the edge point singularities, an improved LP decomposition is used, and a multiscale edge detection algorithm based on Laplacian Pyramid is proposed. This algorithm can detect the image edges reliably and effectively. Subpixei edge location techniques are researched to improve edge location precision. The origin, principle and prerequisite of subpixei edge location are discussed and the current subpixei edge location methods are summarized. As to two step-edge models of one-dimensional and two-dimensional subpixei location, a subpixei edge location algorithm based on Legendre moments is proposed. The parameters' mathematical expressions of subpixei location based on Legendre moments for one-dimensional and two-dimensional edge are respectively deduced. Since three-gray level edge model can better describe actual image edge than two-gray level edge model, the error because of using two-gray level edge model is analyzed and deduced. Then, effects of Gaussian noise on one-dimensional and two-dimensional subpixei edge location are respectively analyzed. Experiments on emulational images and actual images show that this method can efficiently implement subpixei edge location task.

3. The algorithm

The algorithm can be expressed as following equations (1)-(8):

(1) $$f^{(\alpha)}(x_0) = \left.\frac{df(x)}{dx^{\alpha}}\right|_{x=x_0} = \lim_{\delta x \to 0} \frac{\Delta^{\alpha}(f(x) - f(x_0))}{(x - x_0)^{\alpha}},$$

for $0 < a \le 1,$ where

(2) $$\Delta^{\alpha}(f(x) - f(x_0)) \cong \Gamma(1+\alpha) \lim_{x \to \infty} \Delta(f(x) - f(x_0)),$$

and local integral of $f(x)$ defined by

(3) $$ {}_aI_b^{(\alpha)} f(t) = \frac{1}{\Gamma(1+\alpha)} \int_a^b f(t)(dt)^{\alpha} = \frac{1}{\Gamma(1+\alpha)} \lim_{\Delta t \to 0} \sum_{j=0}^{j=N-1} f(t_j)(\Delta t_j)^{\alpha}.$$

Then we get:

$$H_\alpha\{f(t)\} = \hat{f}_H^\alpha(x) = \frac{1}{\Gamma(1+\alpha)} \oint_R \frac{f(t)}{(t-x)^\alpha}(dt)^\alpha, \tag{4}$$

where x is real and the integral is treated as a Canchy principal value, that is

$$\frac{1}{\Gamma(1+\alpha)} \oint_R \frac{f(t)}{(t-x)^\alpha}(dt)^\alpha = \tag{5}$$

$$= \lim_{\varepsilon\to 0}\left[\frac{1}{\Gamma(1+\alpha)} \int_{-\infty}^{x-\varepsilon} \frac{f(t)}{(t-x)^\alpha}(dt)^\alpha + \frac{1}{\Gamma(1+\alpha)} \int_{x+\varepsilon}^{\infty} \frac{f(t)}{(t-x)^\alpha}(dt)^\alpha \right].$$

Rewrite again (4) as

$$\hat{f}_H^\alpha(x) = \frac{1}{\Gamma(1+\alpha)} \int_{-\infty}^{\infty} \frac{f(t)}{(t-x)^\alpha}(dt)^\alpha = \tag{6}$$

$$= \frac{1}{\Gamma(1+\alpha)} \int_{-\infty}^{\infty} f(t)g(x-t)(dt)^\alpha = f(x) * g(x),$$

$$\partial_j(C_{ijkl}\partial_k u_l + e_{kij}\partial_k\varphi) - \rho\ddot{u}_i = 0, \tag{7}$$

$$\partial_j(e_{ijkl}\partial_k u_l - \eta_{kij}\partial_k\varphi) = 0. \tag{8}$$

The linear equation can be expressed into the following simplified forms:

$$L(\nabla,\omega) f(x,\omega) = 0, \tag{9}$$

$$L(\nabla,\omega) = T(\nabla) + \omega^2\rho J,$$

in which,

$$T(\nabla) = \begin{Vmatrix} T_{ik}(\nabla) & t_i(\nabla) \\ t_k^{\mathrm{T}}(\nabla) & -\tau(\nabla) \end{Vmatrix}, \quad J = \begin{Vmatrix} \delta_{ik} & 0 \\ 0 & 0 \end{Vmatrix}, \tag{10}$$

$$f(x,\omega) = \begin{Vmatrix} u_k(x,\omega) \\ \varphi(x,\omega) \end{Vmatrix}.$$

Consider delay, L can be expressed as:

$$L^0 = \begin{Vmatrix} C_{ijkl}^0 & e_{kij}^0 \\ e_{ikl}^{0\mathrm{T}} & -\eta_{ik}^0 \end{Vmatrix}. \tag{11}$$

These functions can be expressed as:

$$C(x) = C^0 + C^1(x), \;\; e(x) = e^0 + e^1(x), \;\; \eta(x) = \eta^0 + \eta^1(x), \tag{12}$$

$$\rho(x) = \rho_0 + \rho_1(x).$$

The value with superscript of 1 represents the difference below:

$$C^1 = C - C^0, \;\; e^1 = e - e^0, \tag{13}$$

$$\eta^1 = \eta - \eta^0, \;\; \rho_1 = \rho - \rho_0,$$

(14) $$f(x,\omega) = f^0(x,\omega) + \int_V S(x-x')(L^1F(y') + \\ +\rho_1\omega^2 g(R)T_1 f(y')]S(y')dy'.$$

In addition, we can introduce the abbreviated formula:

$$g(x,\omega) = \begin{Vmatrix} G_{ik}(x,\omega) & \gamma_i(x,\omega) \\ \gamma_k(x,\omega) & g(x,\omega) \end{Vmatrix}, \quad s(x,\omega) = \begin{Vmatrix} G_{ik,l}(x,\omega) & \gamma_{i,k}(x,\omega) \\ \gamma_{k,l}(x,\omega) & g_{,k}(x,\omega) \end{Vmatrix},$$

(15) $$L^1(x,\omega) = \begin{Vmatrix} C^1_{ijkl} & e^1_{kij} \\ e^{1T}_{kij} & -\eta^1_{ik} \end{Vmatrix}, \quad F(x,\omega) = \begin{Vmatrix} u_{(i,j)}(x,\omega) \\ \varphi_{,i}(x,\omega) \end{Vmatrix}.$$

In these expression, $G_{ik}(x,\omega)$, $\gamma_i(x,\omega)$, $g(x,\omega)$ can be represented as:

$$g(x,\omega) = \frac{1}{(2\pi)^3}\int g(k,\omega)\exp(-ik\cdot x)dk, \quad g(k,\omega) = \begin{Vmatrix} G_{ik}(k,\omega) & \gamma_i(k,\omega) \\ \gamma_k^{\mathrm{T}}(k,\omega) & g(k,\omega) \end{Vmatrix},$$

$$G_{ik} = (\Lambda_{ik} + \frac{1}{\lambda}h_i h_k^{\mathrm{T}})^{-1}, \quad g = -(\lambda + h_l^{\mathrm{T}}\Lambda_{ij}^{-1}h_j)^{-1}, \quad \gamma_i = \frac{1}{\lambda}h_k^{\mathrm{T}}G_{ki},$$

$$\Lambda_{ik}(k,\omega) = k_j C^0_{ijkl}k_k - \rho_0\omega^2\delta_{il}, \quad h_i(k) = e^0_{kil}k_k k_l, \quad h_l^{\mathrm{T}} = e^{0\mathrm{T}}_{ikl}k_i k_k, \quad \lambda(k) = \eta^0_{ik}k_i k_k,$$

(16) $$\frac{1}{2\pi}\int_{-\infty}^{\infty} e^{-ik_3x_3'}dx_3' = \delta(k_3).$$

Equation (8) can be converted into the following form:

(17) $$f(y,\omega) = f^0(y,\omega) + \int_s S(y-y',\omega)L^1F(y',\omega)dy' + \\ +\rho_1\omega^2\int_s g(y-y',\omega)Jf(y',\omega)dy',$$

in which S is cylinder cross section, $y = (x_1, x_2)$, and

(18) $$g(y-y',\omega) = \frac{1}{(2\pi)^2}\int_0^{\infty}\bar{k}d\bar{k}\int_0^{2\pi} g(\bar{k},\omega)\exp(-i\bar{k}\cdot(y-y'))d\phi, \quad \bar{k} = (k_1, k_2),$$

$$G_{ik}(\bar{k},\omega) = \frac{1}{\rho_0\omega^2}\left[\begin{array}{l} \dfrac{\beta^2}{\bar{k}^2-\beta^2}\theta_{ik} + \bar{k}_i\bar{k}_k\left(\dfrac{1}{\bar{k}^2-\alpha^2} - \dfrac{1}{\bar{k}^2-\beta^2}\right), \\ \\ +m_i m_k\dfrac{\beta_\perp^2}{\bar{k}^2-\beta_\perp^2} \end{array}\right],$$

(19)
$$g_{ik}(\bar{k},\omega) = -\frac{1}{\eta_{11}^0}\frac{1}{\bar{k}^2} + \frac{1}{\rho_0\omega^2}\left(\frac{e_{15}^0}{\eta_{11}^0}\right)^2 \frac{\beta_\perp^2}{\bar{k}^2 - \beta_\perp^2},$$

$$\gamma_i(\bar{k}_i,\omega) = \frac{1}{\rho_0\omega^2}\left(\frac{e_{15}^0}{\eta_{11}^0}\right)^2 \frac{\beta_\perp^2}{\bar{k}^2 - \beta_\perp^2} m_i,$$

in which,

(20)
$$\alpha^2 = \frac{\rho_0\omega^2}{C_{11}^0},\ \alpha^2 = \frac{\rho_0\omega^2}{C_{66}^0},\ \beta_\perp^2 = \frac{\rho_0\omega^2}{C_{44}'},\ C_{44}' = C_{44}^0 + \frac{(e_{15}^0)^2}{\eta_{11}^0}.$$

4. Experimental results and analysis

To evaluate the proposed algorithm, we select four images as examples. The results of the proposed segmentation algorithm are shown in Figs 1, 2, 3 and 4, where in each figure are illustrated respectively the original image, the result by traditional watershed algorithm, the result by final mufti-scale algorithm, the result by the algorithm, the result by the algorithm in [8] and the result by the new algorithm. From Figs 1, 2, 3 and 4 it is obvious to see that the proposed algorithm gives optimal results. The results of the new segmentation algorithm are compared with those of the traditional watershed segmentation algorithm, final mufti-scale gradient segmentation algorithm, the algorithm in [7] and the algorithm in [8], respectively.

The result of the traditional watershed segmentation algorithm suffers from serious over segmentation that makes the result virtually useless.

Since the final mufti-scale gradient algorithm LG(*f*) reduces the effect of the noise, the results look much better than traditional watershed. Nevertheless there are some watershed ridge lines that do not correspond to the objects in which we are interested.

The proposed algorithm overcomes the problems of over segmentation and noise sensitiveness of the traditional watershed segmentation algorithm, so the over segrnentation is almost reduced, and the location of the edges is very accurate.

From Fig. 1, we can see that the watershed ridge lines between the rice grains have completely disappeared in the images that were segmented by the proposed segmentation algorithm and the algorithm, unlike in the cases of traditional watershed segmentation algorithm and final mufti-scale gradient segmentation algorithm, where we can see many closed and connected regions whose boundaries follow the contours of the image that made the image look very messy, especial ly in the case of traditional watershed segmentation algorithm. As for the case of the algorithm in [8] the rice grains almost left without marked.

From Figs 2, 3 and 4 we can find that the traditional watershed, final mufti-scale gradient, and the algorithms in [7, 8] over segment the image and saddle regions, which result in many watershed ridge lines that do not correspond to the objects in which we are interested, while only peak and pit regions appear in the image by the proposed algorithm.

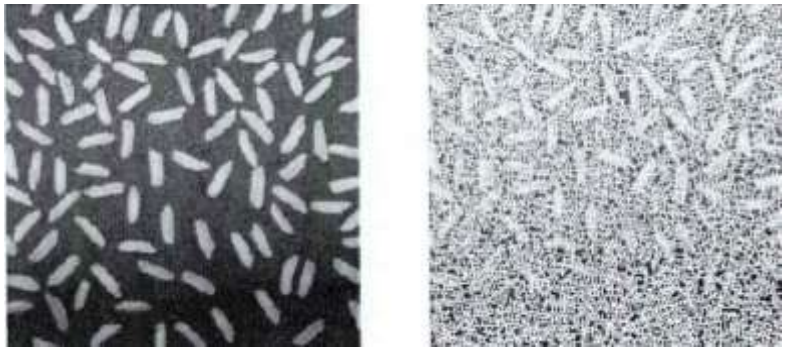

(a) (b)

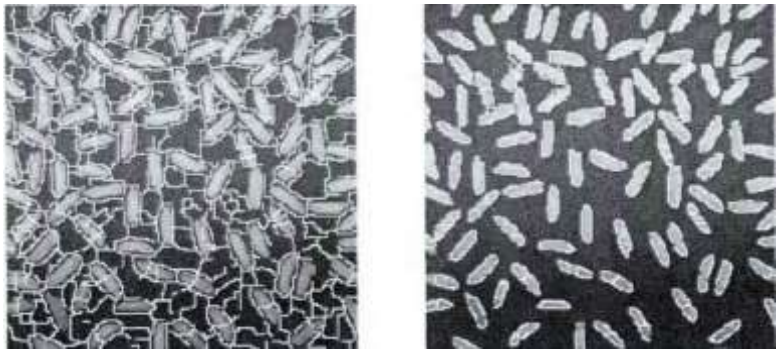

(c) (d)

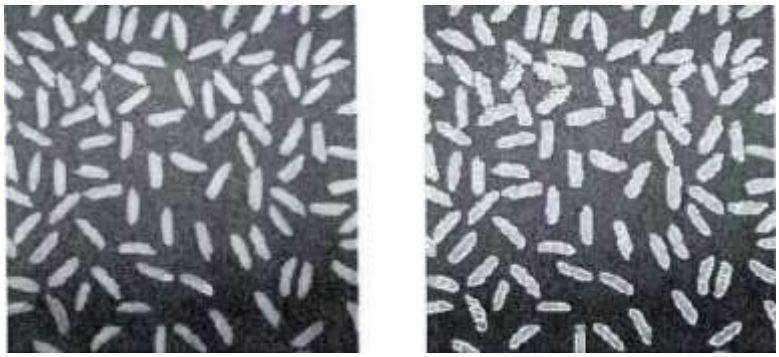

(e) (f)

Fig. 1. Results of edge detection obtained with Rice image: Origin image (a); result of watershed algorithm (b); result of MGA algorithm (c); result of W algorithm (d); result of WT algorithm (e); result of new algorithm (f)

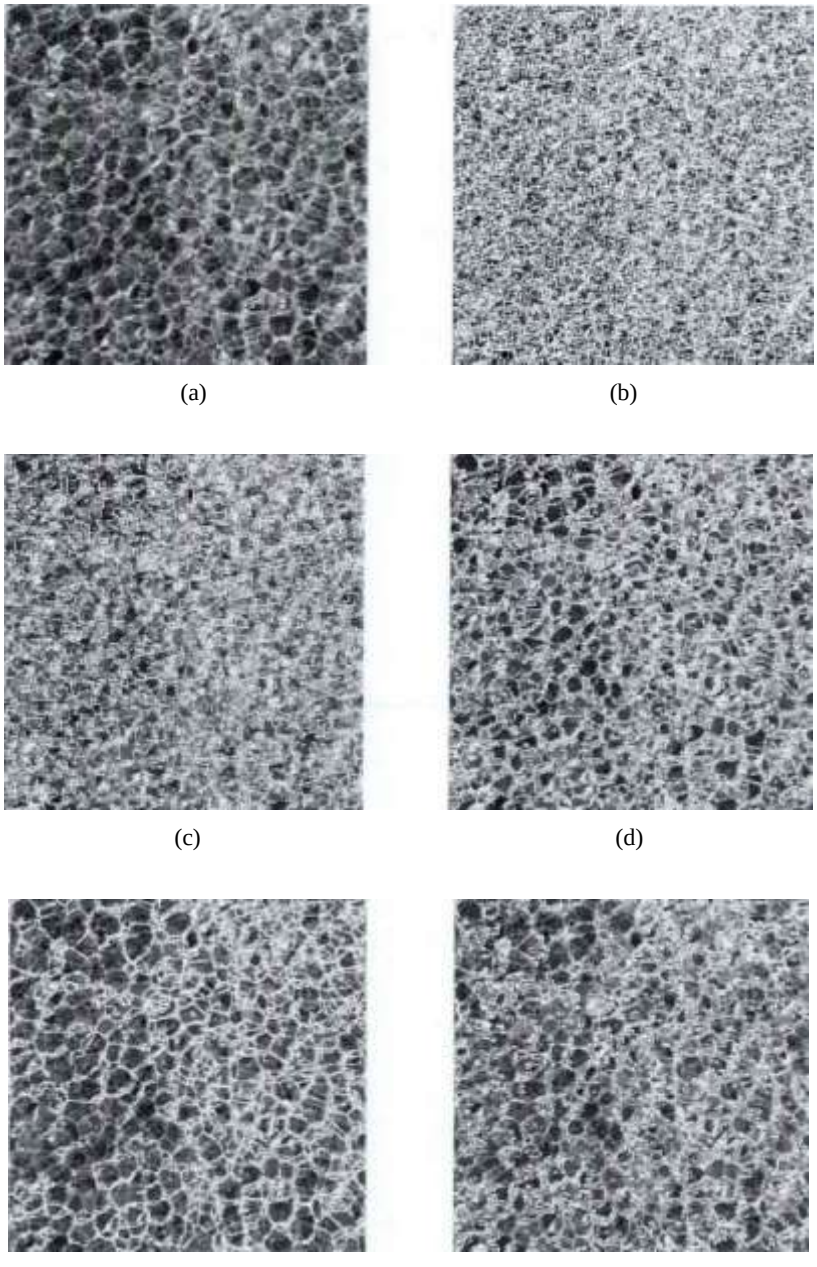

(a) (b)

(c) (d)

(e) (f)

Fig. 2. Results of edge detection obtained with cells image: Origin image (a); result of watershed algorithm (b); result of MGA algorithm (c); result of W algorithm (d); result of WT algorithm (e); result of new algorithm (f)

(a) (b)

(c) (d)

(e) (f)

Fig. 3. Results of edge detection obtained with fingerprint image: Origin image (a); result of watershed algorithm (b); result of MGA algorithm (c); result of W algorithm (d); result of WT algorithm (e); result of new algorithm (f)

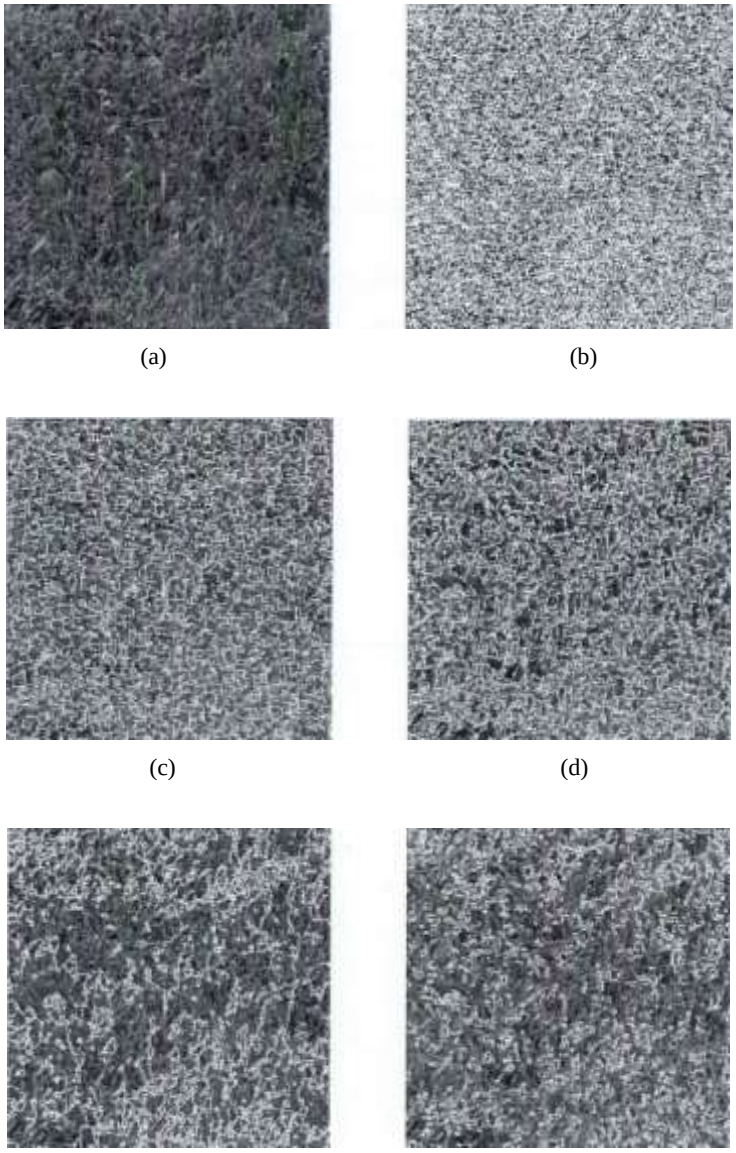

(a) (b)

(c) (d)

(e) (f)

Fig. 4. Results of edge detection obtained with grass image: Origin image (a); result of watershed algorithm (b); result of MGA algorithm (c); result of W algorithm (d); result of WT algorithm (e); result of new algorithm (f)

5. Conclusion

To solve the over segmentation and noise sensitiveness of the simple watershed transform, a new algorithm is proposed in this paper. The proposed segmentation algorithm was implemented in the processing of several images and produced very satisfactory results with respect to suppression of over segmentation. Appropriate

weight function is used to combine the enhanced final mufti-scale gradient algorithm with markers algorithm to get the new algorithm. A combination of these two algorithms can contribute to overcoming the over segmentation and under segmentation which are caused by enhanced final mufti-scale gradient algorithm and markers algorithm respectively. The experimental results show that the new algorithm is superior to the final mufti-scale gradient algorithm, the algorithm in [7] and the algorithm in [8] in terms of suppression of over segmentation of traditional segmentation algorithm.

***Acknowledgements*:** This work was financially supported by Chongqing municipal education commission scientific and technological research project, China (No KJ1503209).

References

1. Zhou, W., X. Du, J. Li. The Limitation of Curvature Gravity Gradient Tensor for Edge Detection and a Method for Overcoming It. – Journal of Applied Geophysics, 2013, pp. 76-82.
2. Ma, G., D. Huang, C. Liu. Application of Balanced Edge Detection Filters to Estimate the Location Parameters of the Causative Sources Using Potential Field Data. – Journal of Applied Geophysics, 2013, pp. 99-106.
3. Chen, W., H. Yue, J. Wang, X. Wu. An Improved Edge Detection Algorithm for Depth Map in Painting. – Optics and Lasers in Engineering, 2014, pp. 203-211.
4. Xu, J., L. Wang, Z. Shi. A Switching Weighted Vector Median Filter Based on Edge Detection. – Signal Processing, 2014, pp. 24-30.
5. Zhang, Y., G. Wang, J. Xu, Z. Shi, DeXing Dong. The Modified Gradient Edge Detection Method for the Color Filter Array Image of the CMOS Image Sensor. – Optics and Laser Technology, 2014, pp. 62-71.
6. Yan, Q., X. Sui. Random Noise Filtering Method Based on the Inter-Frame Registration. – Infrared Physics and Technology, 2014, pp. 67-72.
7. Zhang, H., L. Luo, K. Yang, L. Wang, X. Gao. Improved Multi-Scale Wavelet in Pantograph Slide Edge Detection. – Optik – International Journal for Light and Electron Optics, 2014, pp. 125-129.
8. Yuan, Y., D. Huang, Q. Yu, P. Lu. Edge Detection of Potential Field Data with Improved Structure Tensor Methods. – Journal of Applied Geophysics, 2014, pp. 67-72.